THE JOURNAL OF BIOLOGICAL CHEMISTRY VOL. 287, NO. 42, pp. 35733–35746, October 12, 2012

Deletion of the γ-Aminobutyric Acid Transporter 2 (GAT2 and SLC6A13) Gene in Mice Leads to Changes in Liver and Brain Taurine Contents*

Received for publication, April 1, 2012, and in revised form, August 6, 2012 Published, JBC Papers in Press, August 15, 2012, DOI 10.1074/jbc.M112.368175

Yun Zhou[‡], Silvia Holmseth[‡], Caiying Guo[§], Bjørnar Hassel[¶‖], Georg Höfner[**], Henrik S. Huitfeldt[‡‡], Klaus T. Wanner[**], and Niels C. Danbolt[‡1]

From the [‡]Centre of Molecular Biology and Neuroscience, Department of Anatomy, Institute of Basic Medical Sciences, University of Oslo, N-0317 Oslo, Norway, the [§]HHMI, Janelia Farm Research Campus, Ashburn, Virginia 20147, the [¶]Department for Neurohabilitation, Oslo University Hospital, N-0372 Oslo, Norway, the [‖]Norwegian Defense Research Establishment, N-2027 Kjeller, Norway, the [**]Department für Pharmazie, Zentrum für Pharmaforschung, Ludwig-Maximilians-Universität München, D-81377 München, Germany, and the [‡‡]Department of Pathology, Oslo University Hospital, University of Oslo, N-0372 Oslo, Norway

Background: The physiological roles of GABA transporter 2 (GAT2) are unknown.
Results: Deletion of the GAT2 gene reduced liver taurine levels but increased brain levels.
Conclusion: GAT2 is unimportant for inactivation of neurotransmitter GABA. Instead, GAT2 is a major taurine transporter in hepatocytes and an efflux transporter at the blood-brain barrier.
Significance: GAT2 knockout mice will be crucial for uncovering the roles of GAT2.

The GABA transporters (GAT1, GAT2, GAT3, and BGT1) have mostly been discussed in relation to their potential roles in controlling the action of transmitter GABA in the nervous system. We have generated the first mice lacking the GAT2 (*slc6a13*) gene. Deletion of GAT2 (both mRNA and protein) neither affected growth, fertility, nor life span under nonchallenging rearing conditions. Immunocytochemistry showed that the GAT2 protein was predominantly expressed in the plasma membranes of periportal hepatocytes and in the basolateral membranes of proximal tubules in the renal cortex. This was validated by processing tissue from wild-type and knockout mice in parallel. Deletion of GAT2 reduced liver taurine levels by 50%, without affecting the expression of the taurine transporter TAUT. These results suggest an important role for GAT2 in taurine uptake from portal blood into liver. In support of this notion, GAT2-transfected HEK293 cells transported [^{3}H]taurine. Furthermore, most of the uptake of [^{3}H]GABA by cultured rat hepatocytes was due to GAT2, and this uptake was inhibited by taurine. GAT2 was not detected in brain parenchyma proper, excluding a role in GABA inactivation. It was, however, expressed in the leptomeninges and in a subpopulation of brain blood vessels. Deletion of GAT2 increased brain taurine levels by 20%, suggesting a taurine-exporting role for GAT2 in the brain.

The mammalian genome contains four genes encoding high affinity GABA transporters (GAT1, *slc6a1*; GAT2, *slc6a13*; GAT3, *slc6a11*; and BGT1, *slc6a12* (1, 2)). Most of the interest in these transporters has been in relation to their roles in the inactivation of GABA signaling in the central nervous system (3–5). (Here, we use the GABA transporter nomenclature adopted by the HUGO Gene Nomenclature Committee.) Several studies indicate that GAT1 and GAT3, which are strongly expressed in the brain, account for most of the brain GABA uptake (4, 6–9). In contrast, BGT1 is expressed at low levels in the brain (10) and is concentrated in the leptomeninges rather than in brain tissue proper (11), arguing against a role in controlling GABA receptor activation. Less is known about GAT2. Because neither the exact cellular distribution of GAT2 nor the expression levels have been determined, the literature gives no clues as to a physiological function that can explain why the GAT2 gene is highly conserved among species.

Outside the central nervous system, GABA uptake has been described in liver and kidney *in vivo* (12, 13) and *in vitro* (14, 15), and GABA may play a signaling role in peripheral organs, including the immune system (16, 17). GAT2 is a promising candidate for peripheral GABA uptake (2, 4, 6, 18–23). However, BGT1 has also been shown to be expressed in hepatocytes and in renal collecting ducts (11). Furthermore, as the expression levels of GAT1 and GAT3 have also not been precisely measured in these organs, it is not known which subtype(s) can contribute.

GABA uptake is related to taurine uptake as both GAT2 and TAUT[2] interact with both compounds. The taurine transporter (*slc6a6*), which has high affinity for taurine (K_m 4.5 μM in mouse and K_m 40 μM in rat (24, 25)), can also transport GABA but with low affinity (K_m 1.5 mM (26)). However, GAT2 transports taurine but is classified as a GABA transporter because the affinity for GABA (K_m 18 μM) is considerably higher than that for taurine (K_m 540 μM in rat (2)).

Taurine is a ubiquitously distributed aminosulfonic acid to which several important functions have been ascribed, includ-

* This work was supported by Norwegian Research Council Grant 183727/S10.

[1] To whom correspondence should be addressed: Centre of Molecular Biology and Neuroscience, Dept. of Anatomy, Institute of Basic Medical Sciences, University of Oslo, P. O. Box 1105 Blindern, N-0317 Oslo, Norway. Fax: 47-22-85-12-78; E-mail: n.c.danbolt@medisin.uio.no.

[2] The abbreviations used are: TAUT, taurine transporter; TEMED, *N*,*N*,*N*′,*N*′-tetramethylethylenediamine.

TABLE 1

Antibodies and peptides used to produce them

Species (Sp.) differences between rat (R) and mouse (M) protein sequences are indicated with boldface and underscore. The peptides were made as C-terminal amides except those that represent the actual C terminus. The latter were synthesized as free acids as indicated. Peptides representing GAT2 were synthesized based on the mouse (NP_653095.1) and on the rat (NP_598307.1) protein sequences. The GAT1 (NP_077347) and GAT3 (NP_077348) sequences were the same in mice and rats. The BGT1 peptide was based on the mouse sequence (P31651). The residue numbers are indicated. The antibodies to GAT1 and GAT3 (8, 89) and BGT1 (11) have been described previously.

Antibody no.	Production date	Antibody name	Host (rabbit) no.	Sp.	Residues	Antigen sequence
305	1998-06-21	Anti-GAT1 (584)	68514	M, R	584–599	EQPQAGSSASKEAYI-(free acid)
1050	2009-09-20	Anti-GAT2 (1–40)	K220	M	1–40	M**E**NR**A**SGTTSNGETKPVCP**A**MEKVEEDGTLERE**H**W**N**NKME-(amide)
1068	2009-09-17	Anti-GAT2 (552)	K218	R	552–602	KLRTLKGPLRERLRQLVCPAEDLPQK**S**QPE**L**T**S**PATPMTSLLRLTELESNC-(free acid)
296	1998-04-19	Anti-GAT3 (607)	7D4318	M, R	607–627	CEAKVKGDGTISAITEKETHF-(free acid)
590	2005-12-16	Anti-BGT1 (560)	5B0130	M	560–595	KTQGSFKKRL**R**RLITPDPSLPQPGRR**P**PQDGSSAQN-(amide)

ing antioxidation, osmoregulation, and conjugation of bile acids as well as modulation of neurotransmission and ion movements (27–29). Although TAUT plays a dominant role in taurine transport (30), there are many unresolved issues. For instance, at the blood-brain barrier, there is a taurine-sensitive GABA transport that is hard to attribute to TAUT alone because it is also sensitive to betaine and nipecotic acid (31–37). Deletion of the TAUT gene in mice resulted in dramatic reductions (>80%) in tissue taurine levels in several tissues, including brain, kidney, plasma, and retina, as well as skeletal and heart muscle (30), but immunocytochemistry for taurine suggested that the taurine loss in hepatocytes was only 30% (38). Furthermore, it is not clear whether all of the taurine uptake activity in the liver is due to TAUT, because the liver taurine uptake is more sensitive to competitive inhibition by GABA (39) than is expected from TAUT's low affinity for GABA (26). Taken together, this suggests the existence of an unrecognized taurine transporter at both the blood-brain barrier and in the liver.

To address these issues, we have here, for the first time, generated mice lacking the GAT2 (*slc6a13*) gene. We have also generated a number of antibodies to GAT2 (both to the C and N termini) and used them to identify the locations of GAT2 in tissue sections. The labeling specificity was validated by using tissue deficient in GAT2 as negative controls. Furthermore, we have identified the transporters responsible for GABA and taurine uptake in the liver by using isolated rat hepatocytes and by quantifying the levels of mRNAs encoding GAT1, GAT2, GAT3, BGT1, and TAUT. We confirm that GAT2 is able to transport taurine. Finally, we have measured the tissue contents of amino acids in livers, kidneys, and brains from wild-type and GAT2 knockout mice and find increased taurine levels in the brain and reduced levels in the liver.

EXPERIMENTAL PROCEDURES

Materials—*N*,*N*′-Methylenebisacrylamide, acrylamide, ammonium persulfate, TEMED, and alkaline phosphatase substrates (nitro blue tetrazolium and 5-bromo-4-chloro-3-indolyl phosphate) were from Promega (Madison, WI). SDS of high purity (>99% C12 alkyl sulfate) and bis(sulfosuccinimidyl)suberate, SuperSignal West Dura®, were from Pierce, and electrophoresis equipment were from Hoefer Scientific Instruments (San Francisco). Molecular mass markers for SDS-PAGE, biotinylated anti-rabbit immunoglobulins, nitrocellulose sheets (0.22-μm pores, 100% nitrocellulose), [1,2-^{3}H]taurine (1.15 TBq/mmol), and [2,3-^{3}H]GABA were from Amersham Biosciences. Paraformaldehyde and glutaraldehyde were from TAAB (Reading, UK). DMEM/F-12 (1:1) with GlutaMAX®, fetal bovine serum, nonessential amino acids, and Lipofectamine 2000® were from Invitrogen. All other reagents were obtained from Sigma.

Antibodies—Affinity-purified anti-peptide antibodies were prepared as described (40) by immunizing rabbits with peptides corresponding to N- and C-terminal stretches of GAT2 (Table 1). The antibody Ab1050 (corresponding to the mouse N-terminal residues 1–40) and Ab1068 (corresponding to the rat C-terminal residues 552–602) were used for immunoblotting and for immunocytochemistry except when stated otherwise. Rat antibodies to mouse CD31, which are also known as PECAM-1 (Platelet Endothelial Cell Adhesion Molecule-1), were from Pharmingen (catalog no. 553370; lot 43370). Mouse monoclonal antibodies to glutamine synthetase were from Chemicon (catalog no. MAB302, Billerica, MA). Fluorescein-labeled *Lotus tetragonolobus* lectin (catalog no. FL-1321) and fluorescein-labeled *Dolichos biflorus* agglutinin lectin (catalog no. FL-1031-2) were from Vector Laboratories (Burlingame, CA).

Animals—All animal experimentations were carried out in accordance with the European Communities Council Directive of 24 November 1986 (86/609/EEC). Formal approval to conduct the experiments was obtained from the animal subjects review board of the Norwegian Governmental Institute of Public Health (Oslo, Norway). Care was taken to minimize the number of the experimental animals and to avoid suffering. All animals were fed water *ad libitum*.

Mice (GAT2-fKO) lacking the GAT2 (*slc6a13*) gene were housed in individually ventilated cages at constant temperature (22 ± 0.7 °C) and relative humidity (56 ± 6%) and with water *ad libitum*. The cycle of light was 14 h of light and 10 h of darkness. Cages bedded with Nestpaks™ (Datesand Ltd., Manchester, UK) and enriched with red huts and wooden sticks were changed every 2 weeks. The mice were fed Harlan Teklad 2018, which is a regular unpurified diet rich in taurine (Harland Laboratories Inc., Indianapolis, IN). Young adult male Wistar rats (Møllergaard and Blomhoff, Denmark) weighing 200–220 g were kept on a 12-h light/dark cycle. New Zealand rabbits obtained from B&K Universal (Sollentuna, Sweden) were kept in the animal facility at the Institute of Basic Medical Sciences. Rabbits were immunized and bled as described (40), but they were injected subcutaneously rather than intracutaneously.

Construction and Production of Knockout Animals—The targeting vector was constructed using recombineering technique

described by Liu *et al.* (41). A genomic DNA fragment of 10,891 bp containing exons 4–7 of the gene was retrieved from BAC clone RP23-451N15. A loxP sequence was inserted to intron 4 and an frt-neo-frt-loxP cassette was inserted into intron 7. A fragment of 3,974 bp genomic DNA containing exon 5–7 was floxed and thus created an out of frame deletion after Cre excision (Fig. 1*A*). The targeting vector was electroporated into D1 ES cells, which were derived from F1 hybrid blastocyst of 129S6×C57BL/6J by the Gene Targeting and Transgenic Facility at University of Connecticut Health Center. The G418-resistant ES clones were screened by nested PCR using primers outside the construct paired with primers inside the neo cassette. Chimeric mice were generated by aggregating ES cells with 8-cell embryos of the CD-1 strain. The neo cassette was removed by breeding germ line chimeras with ROSA26FLP1 (Jax stock 003946) homozygous females. The ensuing mice, with LoxP sites in the GAT2 gene, are hereafter referred to as "GAT2-flox" mice. While backcrossing to the C57Bl6 mouse strain, GAT2-flox mice were crossed with Hprt1-Cre (42) mice in the C57Bl6 background. The Hprt1 promotor causes Cre expression and thereby deletion of the GAT2 gene in all cells. The offspring lacking GAT2 completely are hereafter referred to as "GAT2-fKO" mice. These mice have a mixed 129/C57Bl6 genetic background and are in effect conventional knockouts, and they are the mice that have been used in this study. Mice homozygote for the knockout allele (fKO) are hereafter referred to as "knockouts," and mice carrying both the wild-type allele (WT) and the knockout allele are referred to as "heterozygotes," and mice homozygote for the wild-type allele are referred to as "wild types."

Genotyping—Biopsies from ear or tail were proteinase K-digested and subjected to PCR. The primers to detect the GAT2-flox genotype were 5′-cactgagctatcttgctggt-3′ and 5′-ggaacagtttgacaccccaa-3′. The expected PCR products were 262 bp for the wild-type allele and 356 bp for the floxed allele. The primers used to detect the knockout allele after Cre excision were 5′-cactgagctatcttgctggt-3′, 5′-gtcactggctatacgtagct-3′, and 5′-ggaacagtttgacaccccaa. The expected products were 262 bp for the wild-type allele and 379 bp for the knockout allele (Fig. 1, *B* and *C*). Both alleles would be present for a heterozygote.

RNA Isolation, cDNA Synthesis, and TaqMan Assays—Pieces of tissues (5–15 mg) were collected and immediately protected in RNAlater (Ambion), before homogenization and RNA extraction using RNeasy® (Qiagen). The RNA concentration was quantified by using NanoDrop UV spectrometry (NanoDrop Technologies, Wilmington, DE). Two μg of RNA were converted into cDNA by using High Capacity cDNA archive kit. GAT2 expression was measured using TaqMan probes (Mm00446836_m1 and Mm01184315_m1) on a 7900HT Fast Real Time PCR system (Applied Biosystems, Carlsbad, CA). The probes used to detect GAT1, GAT3, BGT1, TAUT, and GAPDH were, respectively, Mm00618601_m1, Mm00556476_ml, Mm00446665_ml, Mm00436909_m1, and Mm03302249_g1.

Electrophoresis and Immunoblotting—Tissue was homogenized in 10–20 volumes of ice-cold water (containing 5 mM EDTA and 1 mM PMSF) and centrifuged (39,000 × *g*, 20 min, 4 °C). The supernatants from this centrifugation contained the water-soluble proteins and are hereafter referred to as "supernatant." Care was taken to keep samples cold and work quickly because some other transporters have been shown to be prone to proteolysis (43, 44). The pellets, containing the water-insoluble proteins, were subsequently solubilized in 1% (w/v) SDS in 10 mM sodium phosphate buffer, pH 7.4 (NaP_i), briefly sonicated, and centrifuged (39,000 × *g*, 20 min, 15 °C). The supernatants from this last centrifugation are hereafter referred to as "pellet." The pellets and the supernatants were then subjected to SDS-PAGE and immunoblotted as described (45).

Immunocytochemistry—Mice (aged 36–92 days) were perfusion-fixed as described before (40). Briefly, they were given a lethal dose of pentobarbital, and after cessation of all reflexes, they were perfusion-fixed for 5 min with a fixative consisting of 4% formaldehyde in NaP_i with or without 0.1% glutaraldehyde as stated. The formaldehyde was produced by depolymerizing paraformaldehyde as described before (40). All experiments were performed using wild-type and GAT2 knockout littermate pairs processed in parallel. The images shown here have been prepared by using the antibodies at concentrations below those that gave rise to labeling in GAT2-deficient tissue. We have recently shown how important this validation is (46, 47). The relevant tissues were collected and immersed in fixative for about 1 h at room temperature. Sections were cut from the fixed unfrozen tissue using a Vibratome 1000 plus® (Vibratome, Bannockburn, UK) (thickness, 50 μm).

Immunoperoxidase labeling was done as described previously (48). The sections were treated (5 min) with 1% hydrogen peroxide in 0.1 M NaP_i to inactivate endogenous peroxidase and then treated (30 min) with 1 M ethanolamine in 0.1 M NaP_i. After being washed in phosphate-buffered saline (135 mM NaCl in 10 mM NaP_i), the sections were incubated for 1 h in Tris-buffered saline (TBS: 300 mM NaCl in 100 mM Tris-HCl buffer, pH 7.4) containing 10% newborn calf serum. Then they were incubated with primary antibodies overnight, followed by biotinylated donkey anti-rabbit Ig (1:100) and streptavidin-biotinylated horseradish peroxidase complex (1:100). The sections were examined and photographed on Zeiss Axioskop 2 plus equipped with AxioCam MRc r1.2 camera (Zeiss, Jena, Germany).

For immunofluorescent labeling (49), the sections were rinsed (three times for 5 min) in TBST (TBS with 0.5% Triton X-100), treated with 1 M ethanolamine in 0.1 M NaP_i for 30 min, washed in TBST, incubated (1 h) in TBST containing 10% newborn calf serum and 3% bovine serum albumin followed by incubation with primary antibodies and finally with secondary antibodies (Alexa Fluor goat anti-rabbit 555, Alexa Fluor goat anti-mouse 488, or Alexa Fluor goat anti-rat 488, Molecular Probes, Eugene, OR) diluted 1:1000. For double labeling in kidney, fluorescently labeled lectins to renal collecting ducts (fluorescein-labeled *Dolichos biflorus* agglutinin) or renal proximal tubules (fluorescein-labeled *Lotus tetragonolobus* lectin) (50) were diluted to 1:300 and added to the secondary antibody solutions. The sections were observed in a Zeiss Axioplan 2 microscope equipped with a Zeiss LSM 5 Pascal confocal scanner head (Zeiss, Jena, Germany). Pinhole size was around 1 area unit, optimized for each wavelength to ensure confocality. Exci-

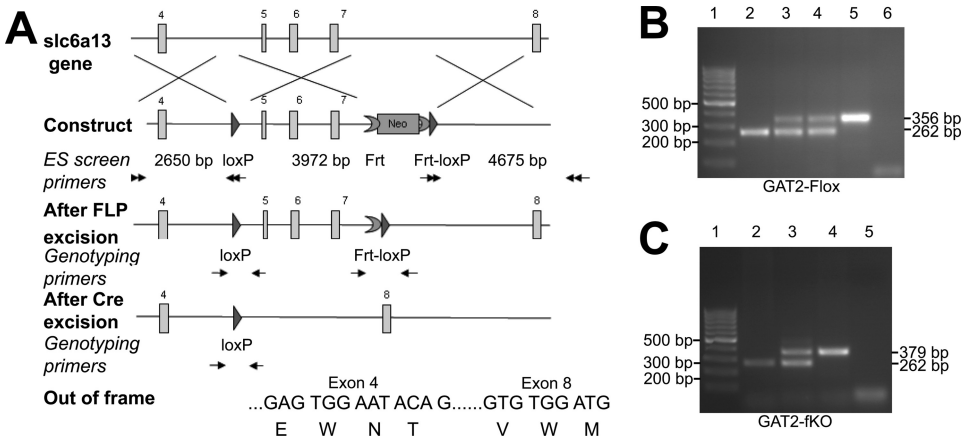

FIGURE 1. **Generation of the GAT2-flox mice.** *A,* gene targeting construct contained exons 4–8 of the GAT2 gene. A loxP sequence (*triangle*) was inserted into intron 4, and a frt-PGKneo-frt-loxP cassette was inserted into intron 7. The lengths of the homologous arms and the floxed fragment are indicated *below* the construct. The *double arrows* indicate the positions of the two sets of nested primers used for ES cell screening. They were located outside the construct and inside the neo cassette. The neo cassette was removed in the GAT2-flox mice generated from chimera × Rosa26FLP crossing. The genotyping primers were indicated by *black arrows below* the *After FLP excision* allele and *After Cre excision* allele. After Cre excision, the DNA encoding amino acid residues 160–277 were deleted. This region is essential for transport activity, and there will be no transport activity without it (87, 88). Furthermore, the deletion causes the remaining sequences to be out of frame. *B,* PCR of genomic DNA to reveal the floxed genotype as follows: 100-bp DNA ladder (*lane 1*); wild-type (*lane 2*); heterozygous GAT2-flox (*lanes 3* and *4*); homozygous GAT2-flox (*lane 5*); and negative control (no DNA) (*lane 6*). *C,* PCR of genomic DNA to identify Cre-mediated recombination (the GAT2-fKO allele) as follows: the 100-bp DNA ladder (*lane 1*), wild-type (*lane 2*), heterozygous (*lane 3*), homozygous knockout (*lane 4*), and negative control (no DNA) (*lane 5*).

tation wavelengths were 488 and 555 with corresponding emission wavelengths at 520 and 568 nm.

[^{3}H]GABA and [^{3}H]Taurine Uptake by Primary Cultures of Rat Hepatocytes—Hepatocytes were isolated from young adult male Wistar rats (200–220 g) and seeded as described previously (51). The cultures were kept in 5% CO_2 at 37 °C. Cell culture medium was removed, and the uptake reaction was started by adding 200 μl of [^{3}H]GABA (50 nM) or [^{3}H]taurine (35 μM) in transport medium (137 mM NaCl, 5 mM KCl, 0.39 mM $NaHCO_3$, 0.44 mM KH_2PO_4, 0.95 mM $CaCl_2$, 0.8 mM $MgSO_4$, 25 mM D-glucose, and 10 mM NaHEPES, pH 7.4). After incubation (37 °C; [^{3}H]GABA, 10 min; [^{3}H]taurine, 25 min), the reaction was terminated by removal of the transport medium and washing two times with 400 μl of ice-cold transport medium. Then 300 μl of 1 M potassium hydroxide was added to the cells (30 min, room temperature), and the cell-associated radioactivity was determined by liquid scintillation counting.

Amino Acid Measurements—For measurements of amino acids, mice were killed by cervical dislocation and decapitation. Livers and brains were rapidly removed and plunged into liquid nitrogen. The tissue samples were weighed in the frozen state and homogenized to a 10% homogenate (w/v) with 3.5% perchloric acid (v/v) containing 1 mM α-aminoadipate as an internal concentration standard. Protein was removed by centrifugation, and samples were neutralized with 9 M potassium hydroxide. The precipitating potassium perchlorate was removed by centrifugation. Amino acids were quantified by HPLC after pre-column derivatization with *o*-phthaldialdehyde as described (52).

Uptake of [^{3}H]Taurine and [^{3}H]GABA by GAT2-transfected HEK293 Cells—HEK293 cells and HEK293 cells stably expressing mouse GAT2 (*slc6a13*) were cultivated as described (53). They were originally referred to as "HEKmGAT3" (53), but to avoid confusion due to GABA transporter nomenclature, we here refer to them as "HEK-GAT2." These cells were grown in 145-cm^2 plates to a confluence of 70–90%, detached by repeated aspiration and discharge of 12 ml of Dulbecco's modified Eagle's medium (DMEM, Sigma), transferred to 50-ml tubes, and pelleted by centrifugation (5 min, 500 × *g*, Biofuge Stratos, Heraeus, Hanau, Germany). The cells were resuspended in the same volume of PBS (137 mM NaCl, 2.7 mM KCl, 8 mM Na_2HPO_4, 1.75 mM KH_2PO_4, pH 7.4) and centrifuged again. After repeating this washing step, the cells were resuspended in Krebs buffer (2.5 mM $CaCl_2$, 1.2 mM $MgSO_4$, 1.2 mM KH_2PO_4, 4.7 mM KCl, 11 mM glucose, 25 mM Tris, 119 mM NaCl with hydrochloric acid adjusted to pH 7.2) or Krebs buffer without Na^+ (2.5 mM $CaCl_2$, 1.2 mM $MgSO_4$, 1.2 mM KH_2PO_4, 4.7 mM KCl, 11 mM glucose, 25 mM Tris, 119 mM choline chloride with hydrochloric acid adjusted to pH 7.2). Uptake assays were performed immediately with aliquots of the resulting cell suspension (about 400,000 cells) in a total volume of 250 μl in 3.5-ml polystyrene tubes (Sarstedt, Nümbrecht, Germany). The cells were equilibrated for 25 min in Krebs buffer in the presence of the test compound at 37 °C in a gently shaking water bath. After addition of 25 μl of 1500 nM [^{3}H]taurine (740 GBq/mmol, Biotrend, Köln, Germany) in Krebs buffer, the cells were incubated for another 10 min. Incubation was stopped by filtration through Whatman GF/C filters pre-soaked for 1 h in 0.9% NaCl by means of a Brandel M-24R harvester. The filters were rinsed with cold 0.9% NaCl and subsequently counted in 3 ml of Rotiszint Eco Plus (Roth, Karlsruhe, Germany) by means of a Packard TriCarb 2300 liquid scintillation counter (PerkinElmer Life Sciences).

Uptake assays with [^{3}H]GABA were performed the same way described above with aliquots of the resulting cell suspension (about 400,000 HEK-GAT2). After a preincubation for 25 min (performed as described for [^{3}H]taurine uptake), 25 μl of a solution containing [^{3}H]GABA (3 TBq/mmol, Biotrend, Köln, Germany) and unlabeled GABA in Krebs buffer (yielding a final concentration of 8 nM [^{3}H]GABA and 32 nM unlabeled GABA in the assay) were added to the cells. Incubation for 4 min was

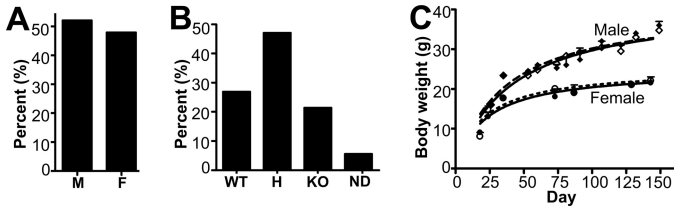

FIGURE 2. **Gender and genotype distributions and growth curves of the GAT2-fKO mice.** *A,* gender distribution (based on 548 mice) was 52.1% males and 47.9% females. *B,* genotype distribution (based on 89 mice) was 26.9% wild types (*WT*), 47.1% heterozygotes (*H*), 21.4% knockouts (*KO*), and 5.6% undetermined (*ND*). Thus, the proportions of WT, heterozygotes, and knockouts were about 1:2:1. *C,* body weights were plotted according to gender and genotype as indicated. The data were based on eight wild-type males, eight knockout males, 9 wild-type females, and 6 knockout females that were followed for 150 days. Note that there were no significant differences between wild-type (*solid lines*) and knockout mice (*dashed lines*).

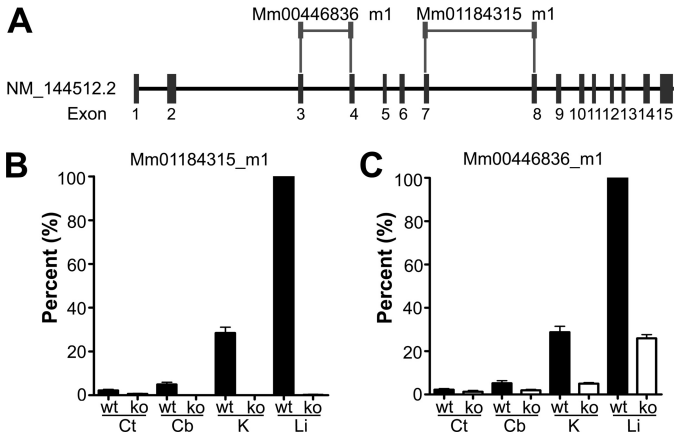

FIGURE 3. **GAT2 mRNA levels in knockout (*ko*) and wild-type (*WT*) animals were measured using TaqMan real time PCR analysis with two different GAT2 probes (Mm01184315_m1 and Mm00446836_m1).** *A,* probe Mm01184315_m1 was directed to a part of the sequence that has been deleted (see Fig. 1*A*), although probe Mm00446836_m1 was to a part still present in the genome. *B* and *C,* two GAT2 probes gave similar results in wild-type (*WT*) mice. The highest GAT2 mRNA levels were found in liver (*Li*) and kidney (*K*), whereas the levels in the cerebellum (*Cb*) and cerebral cortex (neocortex, *Ct*) were low. Note that both the neocortical and cerebellar samples included the surface (pia mater) and that the kidney samples were thin slices from the middle part of intact kidneys thereby containing a small amount of renal medulla surrounded by renal cortex. Also note that the samples from knockout mice gave no signal with the Mm01184315_m1 probe (*C*) but a weak signal with the other probe (*B*) indicating that some of the nonexcised part of the gene was still transcribed, albeit at low levels and with a frameshift (see Fig. 1*A*). The data were based on samples from three pairs of fKO and wild-type littermates (2–3 months old).

stopped by filtration and radioactivity measured as described above. The K_m and K_i values for taurine were calculated from [^{3}H]taurine uptake experiments (according to Ref. 54 for homologous competitive binding curves) and [^{3}H]GABA uptake experiments (according to Ref. 55), respectively.

Data Analysis—Specific uptake in inhibition experiments was defined as the difference between total uptake (without any inhibitor) and nonspecific uptake in the presence of 10 mM β-alanine). The IC_{50} values of the test compounds were calculated from inhibition curves with Prism 4.02 (GraphPad Software, San Diego) using the equation intended for one-site competition. Specific uptake in the absence of any inhibitor was set to 100% (top constraint), whereas nonspecific uptake defined in the presence of 10 mM β-alanine was set to 0% (bottom level constraint).

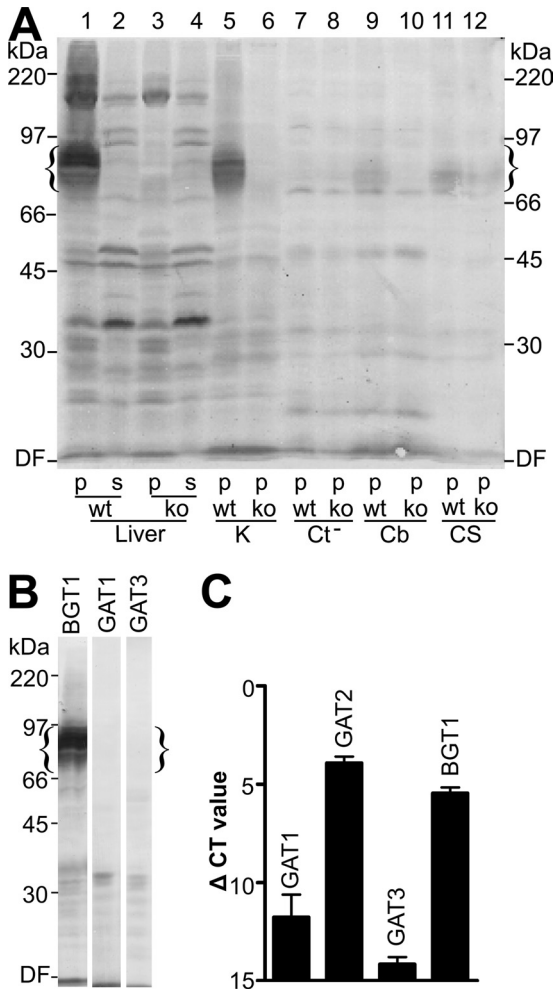

FIGURE 4. **GAT2 expression levels.** *A,* immunoblot showing GAT2 protein (*braces*). Tissue from mice were homogenized in water to separate water-soluble proteins (*s*) from water insoluble proteins (*p*; "pellets") as follows: wild-type (*WT*) liver pellet (*lane 1*); wild-type liver water-soluble proteins (*lane 2*); knockout (*ko*) liver water-soluble proteins (*lane 3*); knockout liver pellet (*lane 4*); wild-type kidney pellet (*lane 5*); knockout kidney pellet (*lane 6*); neocortex pellet without the surface layer (Ct^-) from wild-type (*lane 7*); knockout (*lane 8*); wild-type cerebellum pellet (*lane 9*); knockout cerebellum (*Cb*) pellet (*lane 10*); wild-type neocortical surface (the part removed from *lane 7*) (*lane 11*); and knockout neocortical surface (*CS;* the part removed from *lane 8*) (*lane 12*). Note that this blot had been developed for a long time after *lane 1* reached saturation to let brain GAT2 become visible, and this detection system has a relatively low contrast. Each lane contained 60 μg of protein each. The blot was developed with the C-terminal GAT2-antibody Ab1050 (2 μg/ml), and bound antibodies were detected using alkaline phosphatase-conjugated secondary antibodies and alkaline phosphatase substrates. *B,* immunoblots to detect GABA transporters. *Curly braces* indicate the expected location of transporter bands. 60 μg of protein from liver was loaded. The blots were developed with C-terminal antibodies (0.5 μg/ml) to BGT1 (Ab 590 (11)), GAT1 (Ab 305), and GAT3 (Ab 296), respectively. *C,* levels of mRNA encoding GABA transporters were measured relative to glyceraldehyde phosphate dehydrogenase in mouse liver using TaqMan real time PCR. The *CT* values represent the number of PCR cycles required to reach detection threshold for each GABA transporter subtypes. For example, the difference in ΔCT values between GAT2 and GAT3 was about 10 implying that GAT2 mRNA was present at 2^{10} times higher concentrations. The results were from four independent experiments (means ± S.E.). *DF*, dye front.

RESULTS

Construction of GAT2 Knockout Animals—The GAT2-flox mice were crossed with a general deleter line (Hprt1-Cre; Ref. 42) causing Cre-mediated GAT2 deletion in all cells (Fig. 1*A*). The offspring after this crossing was maintained as heterozy-

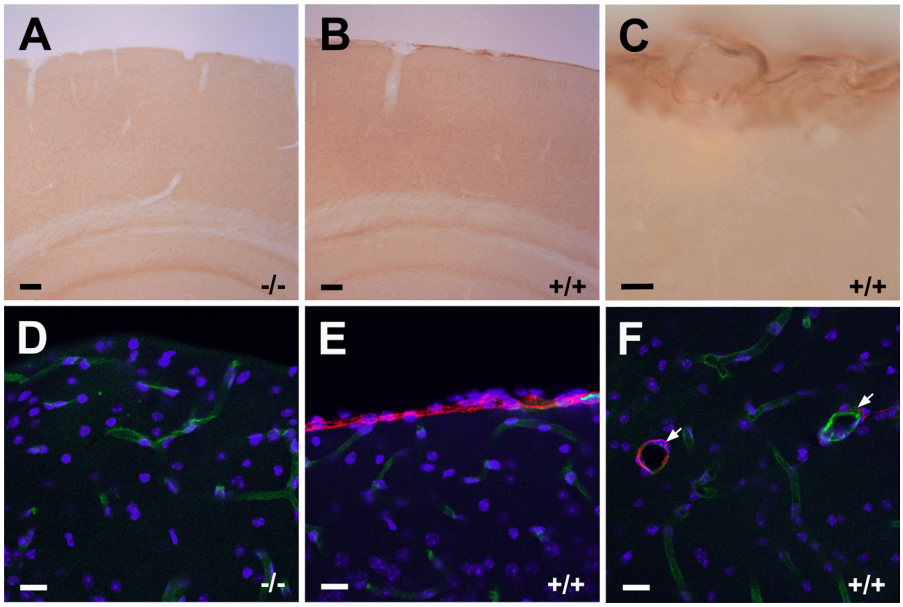

FIGURE 5. **Brain GAT2 is located in the leptomeninges and in some blood vessels.** *A–C,* light micrographs of immunoperoxidase labeled sections from wild-type (*B* and *C*) and knockout (*A*) brain using anti-GAT2 antibodies (Ab1050; 3 μg/ml). *B* and *C* show GAT2 in the leptomeninges. Note that there was a weak but uneven background labeling. Without the negative control that the knockout mice represented, this could easily have been misinterpreted as due to GAT2. *D–F,* confocal micrograph of GAT2 protein in sections from wild-type (*E* and *F*) and knockout (*D*) mice. The sections were labeled with anti-GAT2 antibodies Ab#1050 (*red*; 1 μg/ml) and anti-CD31 antibodies (*green*; 0.5 μg/ml; endothelial marker), and then mounted in DAPI containing medium to visualize the nuclei (*blue*). Note that GAT2 was present in leptomeninges (*E*) and in a subpopulation of small blood vessels (*F, arrowheads*). Fixative, 4% formaldehyde in 0.1 M NaPi, pH 7.4. *Scale bars,* 100 μm in *A* and *B*; 10 μm in *C*; 20 μm in *D–F*.

gotes that were used as breeders to obtain littermates of homozygote mice (knockout and wild-type mice). These mice were first tested using PCR to verify whether the genomic changes worked as intended. DNA from wild-type mice, GAT2-flox mice, and GAT2-fKO mice were collected. As shown (Fig. 1, *B* and *C*), the lengths of the PCR products were as they should be according to the design (Fig. 1*A*).

Breeding and Examination of the Mice—Heterozygous GAT2-fKO (fKO/WT) mice were breeding well, and the knockout mice (fKO/fKO) appeared normal with a normal life span (more than 2 years). The gender distribution was normal (Fig. 2*A*), and the genotype distribution of wild-type, heterozygote, and knockout mice was close to the expected Mendelian ration of 1:2:1 (Fig. 2*B*). Furthermore, the knockout mice were fertile; they gave normal litter sizes (data not shown), and had a growth curve similar to that of wild-type littermate mice (Fig. 2*C*), at least under the normal rearing conditions tested here.

Expression of GABA Transporter mRNAs—To test if GAT2 mRNA was in fact absent, TaqMan real time PCR was used. As shown (Fig. 3, *B* and *C*), GAT2 mRNA was present at relatively high levels in liver and kidney from wild-type mice. There was no significant signal (Fig. 3*B*) in tissue from the knockout mice when using probe Mm01184315_m1, which binds to a part of the sequence that has been deleted (Fig. 1*A*). The other probe that binds to a part upstream from the deleted sequence, did give a weak signal (Fig. 3*C*). This, however, did not give rise to immunoreactivity (Fig. 4*A*) confirming that the knockout construct with a frameshift mutation (Fig. 1*A*) worked as intended. The mRNA levels in whole cerebellum (including leptomeninges and blood vessels) and in kidney were 5.5 $\pm$ 1 and 30 $\pm$ 2%, respectively (means $\pm$ S.E., $n = 4$), of the levels in the liver.

Expression of GABA Transporter Proteins—Consistent with the above data (Fig. 3), the strongest GAT2 labeling (Fig. 4*A*) was obtained with extracts containing membrane proteins from liver (*lane 1*). Note that GAT2 migrated as a broad band (indicated by *braces*) similar to many other transporter proteins, including BGT1 (see Fig. 4*B, below*) and glutamate transporters (56, 57). GAT2 was not detected in any of the water-soluble fractions from wild-type mice (the only one shown is from liver, see Fig. 4*A*, *lane 2*). Furthermore, GAT2 was not detected in samples from the GAT2 knockout mice (Fig. 4*A*, *lanes 3, 4, 6, 8, 10,* and *12*). Also note that bands seen in extracts from the GAT2 knockout or from the water-soluble fractions do not represent GAT2. This blot was developed to detect low level expression and not to obtain a cleanest possible picture.

High GAT2 levels were also found in kidney (Fig. 4*A*, *lane 5*), while the expression levels of GAT2 in brain were low. When neocortical surface was scraped off to obtain sample enriched in the leptomeninges, a weak GAT2 band could be seen on the blots (Fig. 4*A*, *lane 11*). In contrast, the extract from the remaining neocortex did not give any detectable GAT2 signal (Fig. 4*A*, *lane 7*). Extracts from the cerebellum gave a weak GAT2 signal (Fig. 4*A*, *lane 9*), but this may simply be due to larger surface/volume ratio.

To determine whether the liver expressed other proteins with similar functions, Western blots were probed with antibodies to the other GABA transporters. As shown (Fig. 4*B*), BGT1 protein was readily detected in the liver, whereas GAT1 and GAT3 were not. This is in agreement with the mRNA levels in liver (Fig. 4*C*). Note that detection of GAT1 and GAT3 required 8–10 more cycles than detection of GAT2. Assuming comparable affinities of the probes, these data suggested that

GAT1 and GAT3 were expressed at levels that were several hundred times lower than those of GAT2.

Immunocytochemical Localization of GAT2 Protein in Mice—In agreement with the immunoblots, a strong GAT2 signal was detected in the leptomeninges (Fig. 5, *B, C* and *E*), but GAT2 protein was neither detected in brain tissue proper nor in ependymal cells. Some blood vessels, however, expressed GAT2 (Fig. 5*F*). This labeling represented GAT2 because there was no labeling with the GAT2 antibodies in this tissue from knockout littermates processed in parallel (Fig. 5, *A–D*). (The non-GAT2 bands seen in Fig. 4*A* illustrate why it is so important to have tissue from knockout mice as negative controls. For discussion, see Ref. 47.)

In the kidneys, GAT2 immunolabeling was observed in the cortex but not in the medulla. The highest labeling intensity was in the deeper parts of the cortex close to the medulla (Fig. 6, *A, C,* and *D*) in agreement with an earlier report (21). Confocal microscopy revealed that GAT2 was not present at the collecting ducts (Fig. 6*H*) but at the basolateral membranes of parts of proximal tubules (Fig. 6, *F* and *L*). Neither the luminal (brush border) membranes (Fig. 6, *F, H,* and *L*) nor glomeruli and blood vessels were labeled (data not shown). There was no GAT2 labeling in sections from knockout littermates processed in parallel (Fig. 6, *B, E, G, I,* and *K*).

In the liver, strong labeling with the GAT2 antibodies was obtained, but the labeling was not evenly distributed throughout the parenchyma (Fig. 7*A*). Double labeling with antibodies to glutamine synthetase (Fig. 7*B*), which is a marker for perivenous hepatocytes (58), showed that GAT2 was expressed at the highest levels in periportal hepatocytes. (The antibody used here to label glutamine synthetase also labeled endothelial cells.) When sections were double-labeled with antibodies to an endothelial marker (Fig. 7*C*) and to GAT2 (Fig. 7*D*), it was evident that GAT2 was predominantly expressed in hepatocyte plasma membranes (Fig. 7, *D* and *E*). The labeling was not limited to the vascular side but appeared to cover most of the surface of the hepatocytes, although the highest labeling intensity was mostly found at the vascular side (Fig. 7*F*). The endothelium was unlabeled with GAT2 antibodies (Fig. 7*F*). Tissue from GAT2 knockout littermates processed in parallel was GAT2-negative (Fig. 7*G*).

Uptake of [^{3}H]GABA in Isolated Rat Hepatocytes Is Mostly Due to GAT2—As shown above (Fig. 4, *B* and *C*), BGT1 was also present in the liver and at concentrations that were almost as high as those of GAT2. To get more direct information on their contributions to GABA uptake, GABA uptake activity in isolated hepatocytes was measured. The accumulation of [^{3}H]GABA by these cells was dependent on sodium (Fig. 8*B*) and strongly inhibited (Fig. 8*C*) by addition of 1 mM GABA, 1 mM β-alanine, 1 mM (*RS*)-nipecotic acid, or 1 mM hypotaurine. The uptake was virtually unaffected by 1 mM DL-methionine, 1 mM L-cysteine, 1 mM cysteine sulfinic acid, or 1 mM betaine (Fig. 8*C*). Also, this uptake was unaffected by the selective GAT1 inhibitor tiagabine (3 μM) (59). Thus, this substrate selectivity did not match that described for GAT1 and BGT1 because rat GAT1 is highly sensitive to tiagabine and rather insensitive to β-alanine (60–62), and BGT1 is sensitive to betaine and less sensitive to (*RS*)-nipecotic acid (63). Lack of contribution by GAT1 and GAT3 is in agreement with their exceedingly low expression levels in the liver (Fig. 4, *B* and *C*). The minor contribution by BGT1 may in part be due to lower expression levels and in part due to lower affinity for GABA than GAT2 (18). Consequently, it can be concluded that GAT2 is the major contributor for GABA uptake in the liver.

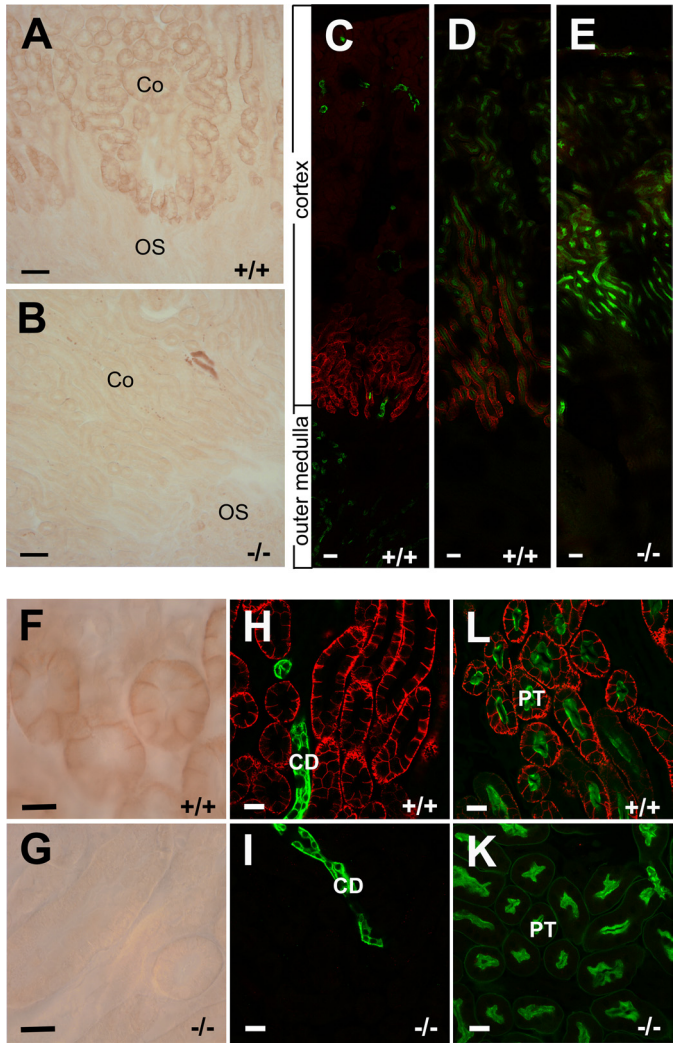

FIGURE 6. **Immunocytochemical visualization of GAT2 protein in kidneys from wild-type (+/+, *A, C, D, F, H,* and *L*) and kidneys from GAT2 knockout (−/−, *B, E, G, I,* and *K*, negative control).** *A* and *B,* low magnification light micrographs of immunoperoxidase-labeled sections from wild-type and knockout mice kidneys (Ab1068; 3 μg/ml). *Scale bars,* 50 μm. *C–E,* montage of multiple confocal micrographs showing GAT2 protein (*red*) in wild-type (*C* and *D*) and knockout (*E*) kidney. The sections were labeled with anti-GAT2 antibodies (*red*; 1 μg/ml) and with either (*C*) fluorescein-labeled *D. biflorus* agglutinin lectin (*green*; 1:300; marker for collecting ducts), or (*D* and *E*) fluorescein-labeled *L. tetragonolobus* Lectin (*green*; 1:300; marker for proximal tubules). Note that GAT2 was located in the deeper parts of the renal cortex close to the medulla. *Scale bars,* 20 μm. *F* and *G,* higher magnification images from the same sections as in *A* and *B*. Note that the labeling (*F*) was in the basolateral membranes and not in the brush border. *Scale bars,* 10 μm. *H, L, I,* and *K,* confocal micrographs of GAT2 protein at the border between the cortex and outer medulla. *H* and *I* were obtained from the sections that were stained with fluorescein-labeled *D. biflorus* agglutinin lectin (*green*; marker for collecting duct), and *L* and *K* were labeled with fluorescein-conjugated *L. tetragonolobus* lectin (*green*; marker for proximal tubules). Note that GAT2 was in the basolateral membranes in proximal tubules. *Scale bars,* 20 μm. For all panels the fixative used was 4% formaldehyde and 0.1% glutaraldehyde in 0.1 M NaP_i, pH 7.4. Abbreviations used are as follows: *Co,* renal cortex; *CD,* collecting duct; *OS,* outer strip of outer medulla; *PT,* proximal tubules.

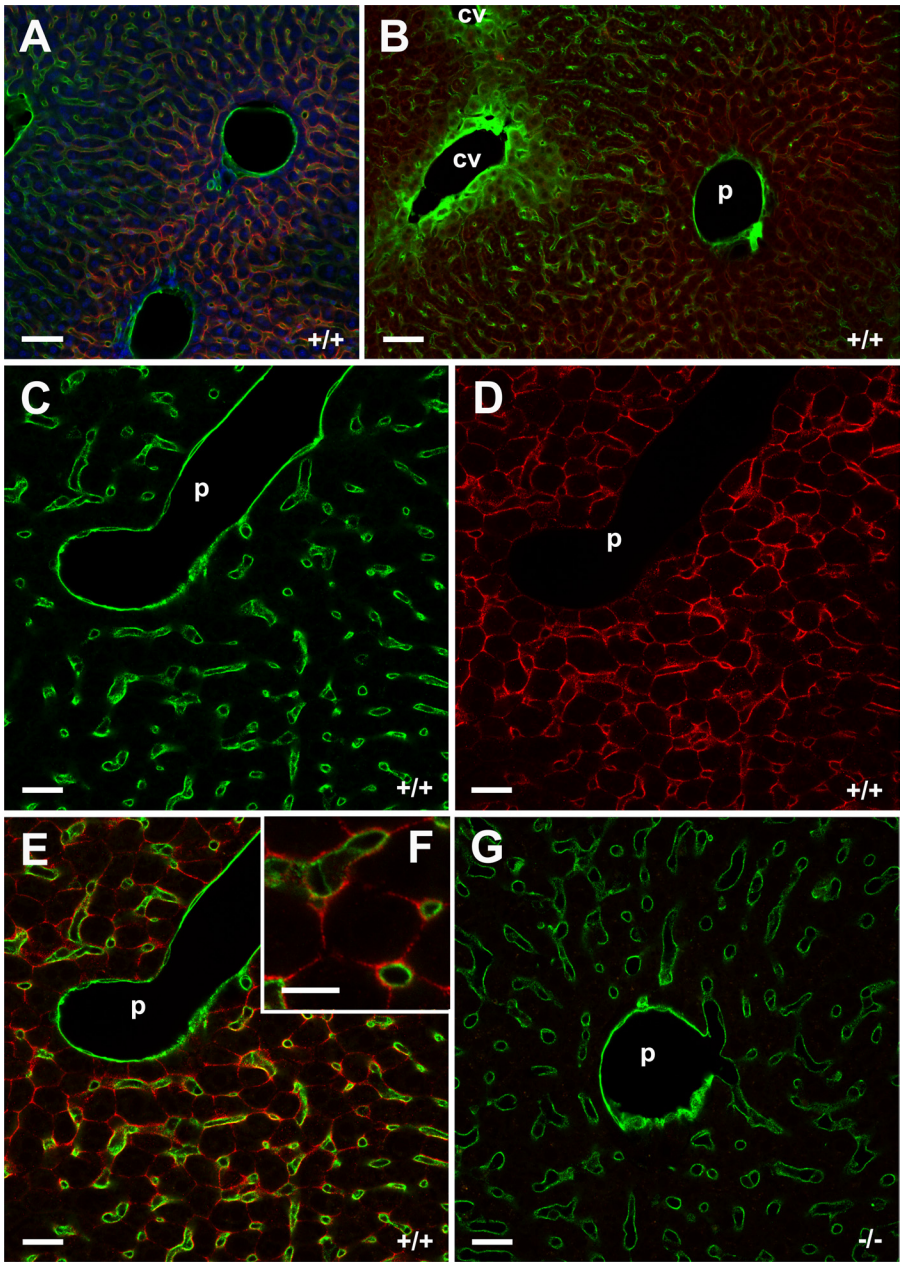

FIGURE 7. **Confocal images of GAT2 protein in mouse liver.** *A* and *B,* periportal labeling of GAT2 in the liver. Low magnification images of sections from wild-type mice which were double labeled with anti-GAT2 antibodies (*red*; Ab1068; 3 μg/ml) and anti-CD31 antibodies (*A, green*; 0.5 μg/ml; endothelial marker) or anti-glutamine synthetase antibodies (*B, green*; 1:500, pericentral hepatocytes marker). *Scale bars,* 50 μm. *C–G,* higher magnification images of sections from wild-type (*C–F*) and knockout (*G*) mice that were double-labeled with anti-GAT2 antibodies (*red*; Ab1068; 3 μg/ml) and anti-CD31 antibodies (*green*; 0.5 μg/ml; endothelial marker). Note that GAT2 was not present in endothelial cells but in the plasma membranes of hepatocytes. *Scale bars,* 20 μm. *p,* portal vein; *cv,* central vein.

Taurine Is a Substrate for GAT2—The inhibition of hepatocyte GABA uptake by nipecotic acid, butyrobetaine, and taurine (Fig. 8*C*) raised the question if GAT2 can transport taurine. This was tested directly (Fig. 9) using GAT2-transfected HEK293 cells (HEK-GAT2). These cells and nontransfected HEK293 cells (negative control) were incubated with [^{3}H]taurine (150 nM) alone or in combination with 10 mM β-alanine, 100 μM (*S*)-SNAP-5114, 100 μM nigericin (ionophore), or 100 μM ouabain (Na^+/K^+-ATPase inhibitor). As shown (Fig. 9*A*) HEK-GAT2 cells were able to take up [^{3}H]taurine in a sodium-dependent manner. Addition of any of the above inhibitors reduced [^{3}H]taurine uptake to sodium-free levels. It was also noted that nontransfected HEK293 had some taurine uptake activity albeit less than those expressing GAT2, but the data did not allow identification of the transporter involved. A low level uptake of taurine has also been described in HeLa cells (64).

Comparison of [^{3}H]Taurine Uptake and [^{3}H]GABA Uptake by GAT2—Inhibition of [^{3}H]taurine and [^{3}H]GABA uptake in HEK-GAT2 by unlabeled taurine and DDPM-1457 ((3*S*)-1-[4,4,4-Tris(4-methoxyphenyl)but-2-en-1-yl]piperidine-3-carboxylic acid), which is a moderately potent mouse GAT2 inhibitor (65), was investigated as described above. Representative inhibition curves indicated that inhibition of [^{3}H]taurine uptake in HEK-GAT2 by nonlabeled taurine (Fig. 9*C*) and

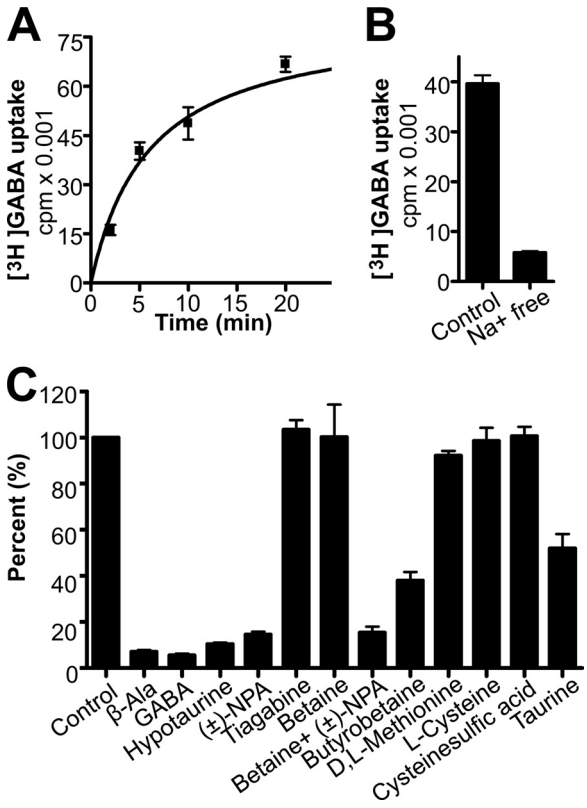

FIGURE 8. **GABA uptake ([^{3}H]GABA, 50 nM) in isolated rat hepatocytes.** *A,* time course (at 37 °C, pH 7.4) of GABA uptake. *B,* GABA uptake was dependent on external sodium ions (incubation time 10 min). Values represent means of one experiment performed in triplicate. *C,* pharmacological effects of the GABA uptake by rat hepatocytes by different drugs (all tested at 1 mM, except tiagabine at 3 μM; incubation time 10 min). The results were given as percent of control uptake measured without inhibitors. The values represent mean ± S.E. (n = 4 independent experiments). Note that the uptake of [^{3}H]GABA was almost completely inhibited by β-alanine, hypotaurine, (*RS*)-nipecotic acid (*NPA*) or GABA, whereas betaine, tiagabine, DL-methionine, L-cysteine, or cysteine sulfinic acid had hardly any effect. Butyrobetaine and taurine inhibited [^{3}H]GABA uptake but was less efficient than β-alanine.

DDPM-1457 (Fig. 9*E*) is in good agreement with inhibition of [^{3}H]GABA uptake by HEK-GAT2 (Fig. 9, *B–D*). The resulting pIC_{50} values (means ± S.E., n = 3) for taurine and DDPM-1457 are shown in Table 2. Furthermore, a K_m value of 210 μM and a K_i value of 220 μM, respectively, could be calculated from the respective IC_{50} values for taurine from these [^{3}H]taurine and [^{3}H]GABA uptake experiments.

Uptake of [^{3}H]taurine in Isolated Rat Hepatocytes Involves Both GAT2 and TAUT at Low External Taurine Concentrations—From the above, it was clear that GAT2 indeed transported taurine. Because previous studies have demonstrated carrier-mediated taurine uptake by isolated rat hepatocytes (66) and attributed this to TAUT (30), we tested the substrate selectivity of the hepatocyte uptake of [^{3}H]taurine (35 μM). The uptake (Fig. 10) was sodium-dependent, and compounds that inhibit both GAT2 and TAUT (1 mM taurine, 1 mM hypotaurine, and 1 mM β-alanine) reduced the [^{3}H]taurine uptake to sodium-free levels. Interestingly, nipecotic acid (which inhibits GAT2 without interacting with TAUT (67, 68)) reduced the sodium-dependent [^{3}H]taurine uptake to about half. Similarly, GABA (0.3 and 1 mM) also reduced the uptake to half in agreement with the fact that GAT2 has high affinity for GABA (K_m 18 μM (2)), whereas TAUT has low affinity (K_m 1.5 mM (26)). This suggested that two transporter proteins, GAT2 and TAUT, were significantly involved in hepatocyte taurine uptake.

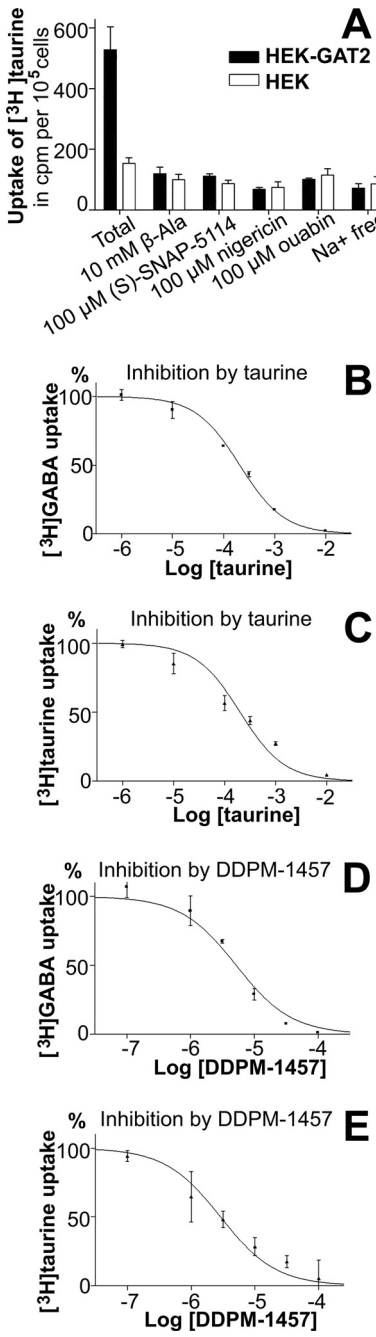

FIGURE 9. **Uptake of [^{3}H]taurine and [^{3}H]GABA by GAT2-transfected HEK293 cells (HEK-GAT2).** *A,* uptake of [^{3}H]taurine by HEK-GAT2 (*slc6a13*; *solid bars*) compared with nontransfected cells (*open bars*). Note that GAT2-transfected cells took up taurine. This uptake was powered by the transmembrane gradient of sodium and was sensitive to inhibition by compounds (β-alanine and SNAP-5114) that were known to inhibit GAT2. The data were from three independent experiments and represented means ± S.D. (n = 6 for total and n = 3 for all others). *B–E,* representative inhibition curves obtained for taurine and DDPM-1457 in [^{3}H]GABA and [^{3}H]taurine uptake experiments employing HEK-GAT2 cells. *B,* inhibition of [^{3}H]GABA uptake by taurine. *C,* inhibition of [^{3}H]taurine uptake by taurine. *D,* inhibition of [^{3}H]GABA uptake by DDPM-1457. *E,* inhibition of [^{3}H]taurine uptake by DDPM-1457. Data points were given as means ± S.D. for triplicate samples. All experiments were performed three times with similar results.

TABLE 2
The pIC_{50} values (means ± S.E., $n = 3$) for taurine and DDPM-1457

	[^{3}H]Taurine uptake (pIC_{50})	[^{3}H]GABA uptake (pIC_{50})
Taurine	3.68 ± 0.13	3.65 ± 0.09
DDPM-1457	5.38 ± 0.08	5.29 ± 0.06

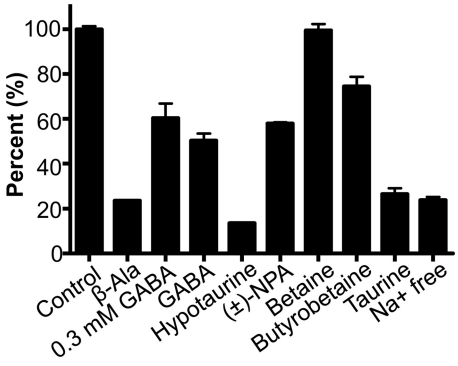

FIGURE 10. **Taurine uptake by isolated rat hepatocytes.** Hepatocytes were incubated (25 min, 37 °C) with 35 μM [^{3}H]taurine alone (*Control*) or in combination with various drugs as indicated. GABA was tested at both 0.3 and 1 mM, whereas the others were tested at 1 mM. Note that the uptake of [^{3}H]taurine was sodium-dependent and that was reduced to sodium-free levels by addition of β-alanine, hypotaurine, or taurine. Betaine had no effect. Note that GABA, butyrobetaine, and (*RS*)-nipecotic acid (*NPA*) reduced [^{3}H]taurine uptake to about half. Values represent mean ± S.E. ($n = 3$).

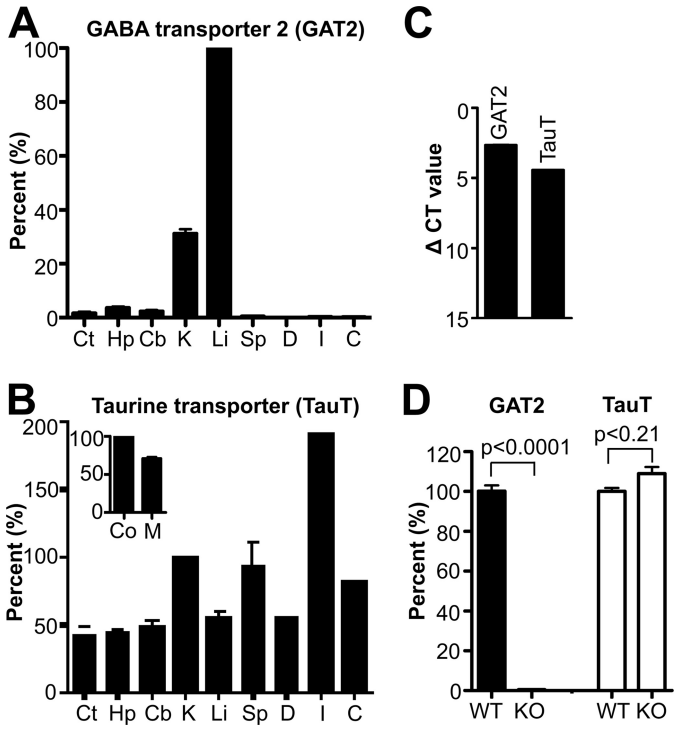

FIGURE 11. **Distributions of GAT2 (*slc6a13*) and taurine transporter (TAUT; *slc6a6*) mRNAs in various organs (*Ct*, neocortex; *Hp*, hippocampus; *Cb*, cerebellum; *K*, kidney; *Li*, liver; *Sp*, spleen; *D*, duodenum; *I*, ileum; *C*, colon) from C57/Bl6 mice (2–3 months old).** *A*, distribution of GAT2 mRNA (mean ± S.E.; $n = 3$ mice) relative to liver using the Mm00446836_m1 probe (Fig. 3). *B*, TAUT mRNA in the same organs relative to the levels in the ileum. The data represent duplicate measurements from one mouse (mean value; the *error bars* represent the highest value). *Inset*, comparison of TAUT mRNA levels (means ± S.E., $n = 3$ mice) in the renal medulla (*M*) and renal cortex (*Co*). *C*, levels of mRNA encoding GAT2 and TAUT relative to GAPDH in mouse liver. Comparison of the GAT2 and the TAUT levels suggested that they were within the same order of magnitude but that the TAUT levels may be slightly lower provided the probes used were equally efficient. *D*, deletion of GAT2 gene did not effect the TAUT mRNA expression. Taqman real time PCRs were used to measure GAT2 mRNA (*solid bars*, Mm01184315_m1) and TauT mRNA (*open bars*, Mm00436909_m1) in the GAT2 wild-type and knockout littermates ($n = 3$).

Organ Distributions of GAT2 and TAUT—Because GAT2 also is able to transport taurine, it became interesting to compare the expression levels and tissue distribution of GAT2 with TAUT (Fig. 11, *A* and *B*). The highest levels of GAT2 (Fig. 11*A*) were found in the liver followed by the kidney. The other organs tested had low levels, including skeletal muscle (data not shown). In contrast, TAUT (Fig. 11*B*) had a wider organ distribution being present at significant levels in all tested organs. The highest levels were found in the ileum followed by the kidney and the spleen. The liver appeared to express somewhat more GAT2 than TAUT (Fig. 11*C*) and provided similar affinities of the two probes. A higher level of GAT2 than TAUT would also be in agreement with the hepatocyte taurine uptake activities (Fig. 10) considering that GAT2 and TAUT took up similar amounts of taurine despite the differences in affinities.

Changes in Tissue Taurine Content in the GAT2-deficient Mice—To test if GAT2 is involved in taurine uptake *in vivo*, we measured the amino acid contents in livers, kidneys, and brains from wild-type and GAT2 knockout mice by HPLC analysis (Table 3). Alanine, glutamate, glutamine, glycine, and leucine, as well as glutathione (GSH), were similar in tissues from wild-type and GAT2-deficient mice. Brain GABA levels were also the same. In contrast, the taurine levels were significantly altered in the liver and in the brain. The GAT2 knockout mice had only half as much taurine in their livers as their wild-type littermates. In the brain, it was the other way around; the taurine levels in the brain were slightly, but significantly, elevated in the GAT2-deficient mice.

Deletion of the GAT2 Gene Did Not Down-regulate TAUT—As deletion of one gene may affect the expression of another, we compared the TAUT mRNA levels in livers from wild-type and GAT2-deficient mice using TaqMan Real Time PCR to check whether the loss of taurine was simply due to the reduction of TAUT. Clearly, the TAUT levels were not reduced in the GAT2 knockout mice (Fig. 11*D*). There were also no significant changes in the levels of GAT1, GAT3, and BGT1 (data not shown).

DISCUSSION

GAT2 Is the Major Taurine Transporter in Hepatocytes at Normal Plasma Taurine Levels—Taurine is ubiquitously distributed in the body and is present at a high concentration in animal tissues (27, 28), and taurine-deficient diets cause significant reduction of tissue taurine levels (69), suggesting that uptake of taurine from the gut is quantitatively more important than synthesis from taurine precursors. In agreement with this notion and with the wide distribution of TAUT (Fig. 11) (24, 25), TAUT-deficient mice exhibited severe taurine deficiency (80–98% loss of taurine) in multiple organs (including the brain, retina, kidney, skeletal muscle, and heart). However, the reduction of taurine in hepatocytes was only about 30% (38). The data we present here offer an explanation; GAT2 is a major taurine transporter in hepatocytes. This conclusion is based on the observations that GAT2-deficient mice had reduced liver

TABLE 3

The amino acid profile between wild-type (+/+) and GAT2 knockout (−/−) tissues

HPLC analysis of tissue components (nmol/mg tissue). The GAT2 knockout mice ($n = 4$; three of which were females) were statistically different from wild-type mice ($n = 6$; five of which were females) with respect to taurine levels in the liver ($p < 0.0063$) and in the brain ($p < 0.0057$). The ages of the mice were 123–138 days. GABA was below detection limit (ND) in liver and kidney.

	Liver		Kidney		Brain	
	+/+	−/−	+/+	−/−	+/+	−/−
GSH	3.0 ± 0.3	3.4 ± 0.4	0.9 ± 0.4	0.8 ± 0.7	0.85 ± 0.03	0.8 ± 0.1
Asp	0.5 ± 0.2	0.6 ± 0.1	2.0 ± 0.4	2.1 ± 0.6	3.2 ± 0.2	3.3 ± 0.3
Glu	1.8 ± 0.8	2.0 ± 0.9	5.4 ± 0.8	6 ± 2	13 ± 1	12 ± 1
Gln	4.0 ± 0.8	4.6 ± 0.6	1.6 ± 0.4	1.5 ± 0.4	6.3 ± 0.6	6.1 ± 0.8
Gly	2.5 ± 0.6	2.8 ± 0.8	6 ± 3	5 ± 2	2.7 ± 0.3	2.4 ± 0.09
Tau	**17 ± 2**	**9 ± 5**	10 ± 2	10 ± 0.6	**8.0 ± 0. 2**	**9.8 ± 0.8**
Ala	4 ± 1	3 ± 1	1.6 ± 0.3	1.4 ± 0.3	1.1 ± 0.08	1.0 ± 0.2
Leu	0.2 ± 0.08	0.16 ± 0.04	0.15 ± 0.05	0.13 ± 0.03	0.014 ± 0.009	0.007 ± 0.002
GABA	ND	ND	ND	ND	2.7 ± 0.1	2.7 ± 0.3

taurine levels and that GAT2 is expressed in hepatocytes and can transport taurine. Furthermore, deletion of GAT2 did not induce major changes in TAUT expression. Finally, with the exception of hypotaurine, GAT2 cannot transport compounds required for taurine synthesis (*e.g.* DL-methionine, L-cysteine, and cysteine sulfinic acid). In fact, GAT2 is predominantly expressed in the periportal region. In contrast, both the transport system for cysteine (70) and cysteine dioxygenase (71, 72), which is one of the key enzymes in taurine biosynthesis, are localized in perivenous hepatocytes. Thus, the hepatocytes with the highest capacity for taurine synthesis are not those with the highest GAT2 levels. Consequently, the reduced taurine content is due to reduced uptake rather than to reduced synthesis.

The experiments shown (Fig. 10) suggested that GAT2 and TAUT contributed equally to taurine uptake. However, at the substrate concentrations used (35 μM), TAUT was fully saturated (given the K_m of 4.5 μM in mouse (24)), whereas GAT2 was operating at a fraction of its capacity (given the K_m values of 200–500 μM). This is relevant because the normal taurine concentrations in plasma are at around 400 μM (28) implying that GAT2 can be expected to dominate hepatic taurine uptake at physiological concentrations.

Most of the GABA Uptake by Hepatocytes Is Catalyzed by GAT2—This study agrees with previous reports that uptake of GABA in the liver is predominantly due to GAT2 (12–14). First, the substrate selectivity matches that of GAT2. Second, the two other high affinity GABA transporters (GAT1 and GAT3) are not significantly expressed in the liver. Third, BGT1 is present in the liver (11) but has lower affinity for GABA (2, 18, 73, 74).

The level of GABA in liver tissue was low probably because the liver does not synthesize GABA (75), but rather it metabolizes GABA (76–78) taken up from the blood. In fact, the GABA concentration in portal venous blood is significantly higher than that in arterial blood (79), and whole body autoradiography following injection of radioactively labeled GABA shows that most of the GABA is taken up by the liver (12, 13). Together, this suggests that the liver is the primary organ responsible for GABA clearance from systemic circulation and that GAT2 is the transporter involved.

It is not known at present how important it is to keep the plasma levels of GABA low, but it may be important if GABA indeed has a signaling role in the immune system and in other peripheral organ systems as suggested (16, 17). The GAT2 knockout mouse produced here may be a good model for testing this hypothesis.

GAT2 May Function as a Brain-to-Blood Efflux System for Taurine—Most of the taurine in the brain is believed to have been acquired by means of uptake from blood plasma rather than having been synthesized locally (27). The brain has also been reported to be able to release taurine (and GABA) to the blood via a sodium-dependent transport system that is sensitive to inhibition by taurine, β-alanine, and GABA (31, 35, 37). We now know that these compounds inhibit not only TAUT but also GAT2.

Considering this, it is striking that deletion of GAT2 resulted in increased taurine levels in the brain (as shown here), although deletion of TAUT resulted in a dramatic reduction (30). This suggests that the two transporters play different roles in the brain. Their distributions are also different. Although high resolution immunocytochemical data are not available for TAUT, it seems clear that TAUT is expressed at fairly high levels in brain parenchyma (80, 81). This is in contrast to GAT2, which is restricted to the blood-brain barrier (leptomeninges and in some cerebral blood vessels as shown here). Based on the above, it seems legitimate to propose that the brain is taking up taurine by means of TAUT and is secreting taurine by means of GAT2.

Role of GAT2 in Controlling Transmitter GABA Seems Unlikely—Although the levels of GAT2 in the brain are believed to be low (2), the contribution of GAT2 to the inactivation of GABA has not been determined due to the difficulties in localizing proteins expressed at low levels without access to knockout animals (see Discussion in Ref. 47). Here, we sort this out by quantifying mRNA and by using several GAT2 antibodies in combination with GAT2 knockout mice. We conclude that cerebral GAT2 is confined to the leptomeninges and to some large blood vessels. This argues strongly against a role of GAT2 in controlling extracellular GABA levels and thereby GABA receptor activation in the adult brain for several reasons. First, GAT1 (82) and GAT3 (21) are expressed at levels that are orders of magnitude higher than those of GAT2 (2, 4, 10, 11). Second, sub-millisecond transmitter removal requires more vacant binding sites (transporter molecules) than released neurotransmitter molecules (57, 83). This explains why GAT1 (82) and GLT1 (84–86) are expressed at such high levels in the brain.

GAT2 Is Unlikely to Take Up Amino Acids from the Glomerular Filtrate—The kidney is, beside the liver, the organ where GAT2 is expressed at the highest levels. Interestingly, GAT2 is not targeted to the brush border but instead to the basolateral membranes. This suggests that GAT2 interacts with the interstitial fluid (and thereby blood plasma) rather than with the glomerular filtrate. Further studies are needed to identify the exact roles of GAT2 in the kidney.

Conclusions—This study is the first report on the creation of GAT2 knockout mice and provides an overview of GAT2 expression levels and localizations as follows. (*a*) GAT2 is predominantly a liver protein, and it is a major taurine transporter in hepatocytes. It also appears to be the major mechanism for maintaining low GABA levels in blood plasma. This may be important if GABA indeed acts as a peripheral signaling molecule (16, 17). (*b*) GAT2 is not likely to be involved in neurotransmitter inactivation in the brain, but GAT2 at the blood-brain barrier may be an efflux transporter for brain taurine. Studies are under way to test if GAT2 is important for brain osmoregulation. (*c*) Considering the fairly high expression levels in proximal tubules, it is plausible that GAT2 plays an as yet unidentified role in the renal handling of taurine. (*d*) The GAT2 knockout mouse described here will be a good model for studies of the physiological and pathophysiological roles of GAT2.

Acknowledgments—We thank Henriette Danbolt for technical assistance and Shuzheng Liu for preparing the hepatocyte primary cultures.

REFERENCES

1. Guastella, J., Nelson, N., Nelson, H., Czyzyk, L., Keynan, S., Miedel, M. C., Davidson, N., Lester, H. A., and Kanner, B. I. (1990) Cloning and expression of a rat brain GABA transporter. *Science* **249,** 1303–1306
2. Liu, Q. R., López-Corcuera, B., Mandiyan, S., Nelson, H., and Nelson, N. (1993) Molecular characterization of four pharmacologically distinct γ-aminobutyric acid transporters in mouse brain (corrected). *J. Biol. Chem.* **268,** 2106–2112
3. Gadea, A., and López-Colomé, A. M. (2001) Glial transporters for glutamate, glycine, and GABA. II. GABA transporters. *J. Neurosci. Res.* **63,** 461–468
4. Conti, F., Minelli, A., and Melone, M. (2004) GABA transporters in the mammalian cerebral cortex. Localization, development, and pathological implications. *Brain Res. Brain Res. Rev.* **45,** 196–212
5. Eulenburg, V., and Gomeza, J. (2010) Neurotransmitter transporters expressed in glial cells as regulators of synapse function. *Brain Res. Rev.* **63,** 103–112
6. Evans, J. E., Frostholm, A., and Rotter, A. (1996) Embryonic and postnatal expression of four γ-aminobutyric acid transporter mRNAs in the mouse brain and leptomeninges. *J. Comp. Neurol.* **376,** 431–446
7. Chiu, C. S., Brickley, S., Jensen, K., Southwell, A., Mckinney, S., Cull-Candy, S., Mody, I., and Lester, H. A. (2005) GABA transporter deficiency causes tremor, ataxia, nervousness, and increased GABA-induced tonic conductance in cerebellum. *J. Neurosci.* **25,** 3234–3245
8. Lee, T. S., Bjørnsen, L. P., Paz, C., Kim, J. H., Spencer, S. S., Spencer, D. D., Eid, T., and de Lanerolle, N. C. (2006) GAT1 and GAT3 expression are differently localized in the human epileptogenic hippocampus. *Acta Neuropathol.* **111,** 351–363
9. Henjum, S., and Hassel, B. (2007) High affinity GABA uptake and GABA-metabolizing enzymes in pig forebrain white matter. A quantitative study. *Neurochem. Int.* **50,** 365–370
10. Lehre, A. C., Rowley, N. M., Zhou, Y., Holmseth, S., Guo, C., Holen, T., Hua, R., Laake, P., Olofsson, A. M., Poblete-Naredo, I., Rusakov, D. A., Madsen, K. K., Clausen, R. P., Schousboe, A., White, H. S., and Danbolt, N. C. (2011) Deletion of the betaine-GABA transporter (BGT1; *slc6a12*) gene does not affect seizure thresholds of adult mice. *Epilepsy Res.* **95,** 70–81
11. Zhou, Y., Holmseth, S., Hua, R., Lehre, A. C., Olofsson, A. M., Poblete-Naredo, I., Kempson, S. A., and Danbolt, N. C. (2012) The betaine-GABA transporter (BGT1, *slc6a12*) is predominantly expressed in the liver and at lower levels in the kidneys and at the brain surface. *Am. J. Physiol. Renal Physiol.* **302,** F316–F328
12. Kuroda, E., Watanabe, M., Tamayama, T., and Shimada, M. (2000) Autoradiographic distribution of radioactivity from [^{14}C]GABA in the mouse. *Microsc. Res. Tech.* **48,** 116–126
13. Hespe, W., Roberts, E., and Prins, H. (1969) Autoradiographic investigation of the distribution of [^{14}C]GABA in tissues of normal and aminooxyacetic acid-treated mice. *Brain Res.* **14,** 663–671
14. Minuk, G. Y., Vergalla, J., Ferenci, P., and Jones, E. A. (1984) Identification of an acceptor system for γ-aminobutyric acid on isolated rat hepatocytes. *Hepatology* **4,** 180–185
15. Goodyer, P. R., Rozen, R., and Scriver, C. R. (1985) A γ-aminobutyric acid-specific transport mechanism in mammalian kidney. *Biochim. Biophys. Acta* **818,** 45–54
16. Young, S. Z., and Bordey, A. (2009) GABA's control of stem and cancer cell proliferation in adult neural and peripheral niches. *Physiology* **24,** 171–185
17. Gavish, M., Bachman, I., Shoukrun, R., Katz, Y., Veenman, L., Weisinger, G., and Weizman, A. (1999) Enigma of the peripheral benzodiazepine receptor. *Pharmacol. Rev.* **51,** 629–650
18. Borden, L. A., Smith, K. E., Hartig, P. R., Branchek, T. A., and Weinshank, R. L. (1992) Molecular heterogeneity of the γ-aminobutyric acid (GABA) transport system. Cloning of two novel high affinity GABA transporters from rat brain. *J. Biol. Chem.* **267,** 21098–21104
19. Durkin, M. M., Smith, K. E., Borden, L. A., Weinshank, R. L., Branchek, T. A., and Gustafson, E. L. (1995) Localization of messenger RNAs encoding three GABA transporters in rat brain. An *in situ* hybridization study. *Brain Res. Mol. Brain Res.* **33,** 7–21
20. Conti, F., Zuccarello, L. V., Barbaresi, P., Minelli, A., Brecha, N. C., and Melone, M. (1999) Neuronal, glial, and epithelial localization of γ-aminobutyric acid transporter 2, a high affinity γ-aminobutyric acid plasma membrane transporter, in the cerebral cortex, and neighboring structures. *J. Comp. Neurol.* **409,** 482–494
21. Jursky, F., and Nelson, N. (1999) Developmental expression of the neurotransmitter transporter GAT3. *J. Neurosci. Res.* **55,** 394–399
22. Minelli, A., Barbaresi, P., and Conti, F. (2003) Postnatal development of high affinity plasma membrane GABA transporters GAT-2 and GAT-3 in the rat cerebral cortex. *Brain Res. Dev. Brain Res.* **142,** 7–18
23. Borden, L. A. (1996) GABA transporter heterogeneity: pharmacology and cellular localization. *Neurochem. Int.* **29,** 335–356
24. Liu, Q. R., López-Corcuera, B., Nelson, H., Mandiyan, S., and Nelson, N. (1992) Cloning and expression of a cDNA encoding the transporter of taurine and β-alanine in mouse brain. *Proc. Natl. Acad. Sci. U.S.A.* **89,** 12145–12149
25. Smith, K. E., Borden, L. A., Wang, C. H., Hartig, P. R., Branchek, T. A., and Weinshank, R. L. (1992) Cloning and expression of a high affinity taurine transporter from rat brain. *Mol. Pharmacol.* **42,** 563–569
26. Tomi, M., Tajima, A., Tachikawa, M., and Hosoya, K. (2008) Function of taurine transporter (Slc6a6/TauT) as a GABA-transporting protein and its relevance to GABA transport in rat retinal capillary endothelial cells. *Biochim. Biophys. Acta* **1778,** 2138–2142
27. Huxtable, R. J. (1989) Taurine in the central nervous system and the mammalian actions of taurine. *Prog. Neurobiol.* **32,** 471–533
28. Brosnan, J. T., and Brosnan, M. E. (2006) The sulfur-containing amino acids. An overview. *J. Nutr.* **136,** 1636S-1640S
29. Ito, T., Schaffer, S. W., and Azuma, J. (2012) The potential usefulness of taurine on diabetes mellitus and its complications. *Amino Acids* **42,** 1529–1539
30. Warskulat, U., Heller-Stilb, B., Oermann, E., Zilles, K., Haas, H., Lang, F., and Häussinger, D. (2007) Phenotype of the taurine transporter knock-out mouse. *Methods Enzymol.* **428,** 439–458
31. Takanaga, H., Ohtsuki, S., Hosoya, Ki., and Terasaki, T. (2001) GAT2/

BGT-1 as a system responsible for the transport of γ-aminobutyric acid at the mouse blood-brain barrier. *J. Cereb. Blood Flow Metab.* **21,** 1232–1239
32. Zhang, Y., and Liu, G. Q. (1998) Sodium and chloride-dependent high and low affinity uptakes of GABA by brain capillary endothelial cells. *Brain Res.* **808,** 1–7
33. Kang, Y. S., Ohtsuki, S., Takanaga, H., Tomi, M., Hosoya, K., and Terasaki, T. (2002) Regulation of taurine transport at the blood-brain barrier by tumor necrosis factor-α, taurine, and hypertonicity. *J. Neurochem.* **83,** 1188–1195
34. Ohtsuki, S. (2004) New aspects of the blood-brain barrier transporters; its physiological roles in the central nervous system. *Biol. Pharm. Bull.* **27,** 1489–1496
35. Lee, N. Y., and Kang, Y. S. (2004) The brain-to-blood efflux transport of taurine and changes in the blood-brain barrier transport system by tumor necrosis factor-α. *Brain Res.* **1023,** 141–147
36. Dominy, J., Eller, S., and Dawson, R., Jr. (2004) Building biosynthetic schools. Reviewing compartmentation of CNS taurine synthesis. *Neurochem. Res.* **29,** 97–103
37. Rasgado-Flores, H., Mokashi, A., and Hawkins, R. A. (2012) Na^+-dependent transport of taurine is found only on the abluminal membrane of the blood-brain barrier. *Exp. Neurol.* **233,** 457–462
38. Warskulat, U., Borsch, E., Reinehr, R., Heller-Stilb, B., Mönnighoff, I., Buchczyk, D., Donner, M., Flögel, U., Kappert, G., Soboll, S., Beer, S., Pfeffer, K., Marschall, H. U., Gabrielsen, M., Amiry-Moghaddam, M., Ottersen, O. P., Dienes, H. P., and Häussinger, D. (2006) Chronic liver disease is triggered by taurine transporter knockout in the mouse. *FASEB J.* **20,** 574–576
39. Inoue, M., and Arias, I. M. (1988) Taurine transport across hepatocyte plasma membranes. Analysis in isolated rat liver sinusoidal plasma membrane vesicles. *J. Biochem.* **104,** 155–158
40. Danbolt, N. C., Lehre, K. P., Dehnes, Y., Chaudhry, F. A., and Levy, L. M. (1998) Localization of transporters using transporter-specific antibodies. *Methods Enzymol.* **296,** 388–407
41. Liu, P., Jenkins, N. A., and Copeland, N. G. (2003) A highly efficient recombineering-based method for generating conditional knockout mutations. *Genome Res.* **13,** 476–484
42. Tang, S. H., Silva, F. J., Tsark, W. M., and Mann, J. R. (2002) A Cre/loxP-deleter transgenic line in mouse strain 129S1/SvImJ. *Genesis* **32,** 199–202
43. Beckstrøm, H., Julsrud, L., Haugeto, O., Dewar, D., Graham, D. I., Lehre, K. P., Storm-Mathisen, J., and Danbolt, N. C. (1999) Interindividual differences in the levels of the glutamate transporters GLAST and GLT, but no clear correlation with Alzheimer disease. *J. Neurosci. Res.* **55,** 218–229
44. Li, Y., Zhou, Y., and Danbolt, N. C. (2012) The rates of post-mortem proteolysis of glutamate transporters differ dramatically between cells and between transporter subtypes. *J. Histochem. Cytochem.* **60,** in press
45. Holmseth, S., Scott, H. A., Real, K., Lehre, K. P., Leergaard, T. B., Bjaalie, J. G., and Danbolt, N. C. (2009) The concentrations and distributions of three C-terminal variants of the GLT1 (EAAT2; *slc1a2*) glutamate transporter protein in rat brain tissue suggest differential regulation. *Neuroscience* **162,** 1055–1071
46. Holmseth, S., Lehre, K. P., and Danbolt, N. C. (2006) Specificity controls for immunocytochemistry. *Anat. Embryol.* **211,** 257–266
47. Holmseth, S., Zhou, Y., Follin-Arbelet, V. V., Lehre, K. P., Bergles, D. E., and Danbolt, N. C. (2012) Specificity controls for immunocytochemistry. The antigen preadsorption test can lead to inaccurate assessment of antibody specificity. *J. Histochem. Cytochem.* **60,** 174–187
48. Lehre, K. P., Levy, L. M., Ottersen, O. P., Storm-Mathisen, J., and Danbolt, N. C. (1995) Differential expression of two glial glutamate transporters in the rat brain. Quantitative and immunocytochemical observations. *J. Neurosci.* **15,** 1835–1853
49. Holmseth, S., Dehnes, Y., Bjørnsen, L. P., Boulland, J. L., Furness, D. N., Bergles, D., and Danbolt, N. C. (2005) Specificity of antibodies. Unexpected cross-reactivity of antibodies directed against the excitatory amino acid transporter 3 (EAAT3). *Neuroscience* **136,** 649–660
50. Phillips, C. L., Miller, K. J., Filson, A. J., Nürnberger, J., Clendenon, J. L., Cook, G. W., Dunn, K. W., Overbeek, P. A., Gattone, V. H., 2nd, and Bacallao, R. L. (2004) Renal cysts of inv/inv mice resemble early infantile nephronophthisis. *J. Am. Soc. Nephrol.* **15,** 1744–1755
51. Skarpen, E., Lindeman, B., Thoresen, G. H., Guren, T. K., Oksvold, M. P., Christoffersen, T., and Huitfeldt, H. S. (2000) Impaired nuclear accumulation and shortened phosphorylation of ERK after growth factor stimulation in cultured hepatocytes from rats exposed to 2-acetylaminofluorene. *Mol. Carcinog.* **28,** 84–96
52. Hassel, B., Bachelard, H., Jones, P., Fonnum, F., and Sonnewald, U. (1997) Trafficking of amino acids between neurons and glia *in vivo*. Effects of inhibition of glial metabolism by fluoroacetate. *J. Cereb. Blood Flow Metab.* **17,** 1230–1238
53. Kragler, A., Höfner, G., and Wanner, K. T. (2008) Synthesis and biological evaluation of aminomethylphenol derivatives as inhibitors of the murine GABA transporters mGAT1–mGAT4. *Eur. J. Med. Chem.* **43,** 2404–2411
54. Motulsky, H., and Christopoulos, A. (2004) *Fitting Models to Biological Data Using Linear and Nonlinear Regression. A Practical Guide to Curve Fitting*, pp. 222–232, Oxford University Press, London
55. Cheng, Y., and Prusoff, W. H. (1973) Relationship between the inhibition constant (K_1) and the concentration of inhibitor which causes 50% inhibition (I_{50}) of an enzymatic reaction. *Biochem. Pharmacol.* **22,** 3099–3108
56. Levy, L. M., Lehre, K. P., Rolstad, B., and Danbolt, N. C. (1993) A monoclonal antibody raised against an ($Na^+ + K^+$)-coupled L-glutamate transporter purified from rat brain confirms glial cell localization. *FEBS Lett.* **317,** 79–84
57. Danbolt, N. C. (2001) Glutamate uptake. *Prog. Neurobiol.* **65,** 1–105
58. Gaasbeek Janzen, J. W., Gebhardt, R., ten Voorde, G. H., Lamers, W. H., Charles, R., and Moorman, A. F. (1987) Heterogeneous distribution of glutamine synthetase during rat liver development. *J. Histochem. Cytochem.* **35,** 49–54
59. Nielsen, E. B., Suzdak, P. D., Andersen, K. E., Knutsen, L. J., Sonnewald, U., and Braestrup, C. (1991) Characterization of tiagabine (NO-328), a new potent and selective GABA uptake inhibitor. *Eur. J. Pharmacol.* **196,** 257–266
60. Borden, L. A., Murali Dhar, T. G., Smith, K. E., Weinshank, R. L., Branchek, T. A., and Gluchowski, C. (1994) Tiagabine, SK&F 89976-A, CI-966, and NNC-711 are selective for the cloned GABA transporter GAT-1. *Eur. J. Pharmacol.* **269,** 219–224
61. Soudijn, W., and van Wijngaarden, I. (2000) The GABA transporter and its inhibitors. *Curr. Med. Chem.* **7,** 1063–1079
62. Kragler, A., Höfner, G., and Wanner, K. T. (2005) Novel parent structures for inhibitors of the murine GABA transporters mGAT3 and mGAT4. *Eur. J. Pharmacol.* **519,** 43–47
63. Borden, L. A., Smith, K. E., Gustafson, E. L., Branchek, T. A., and Weinshank, R. L. (1995) Cloning and expression of a betaine/GABA transporter from human brain. *J. Neurochem.* **64,** 977–984
64. Melamed, N., and Kanner, B. I. (2004) Transmembrane domains I and II of the γ-aminobutyric acid transporter GAT-4 contain molecular determinants of substrate specificity. *Mol. Pharmacol.* **65,** 1452–1461
65. Pabel, J., Faust, M., Prehn, C., Wörlein, B., Allmendinger, L., Höfner, G., and Wanner, K. T. (2012) Development of an (*S*)-1-{2-[tris(4-methoxyphenyl)methoxy]ethyl}piperidine-3-carboxylic acid [(*S*)-SNAP-5114] carba analogue inhibitor for murine γ-aminobutyric acid transporter type 4. *ChemMedChem* **7,** 1245–1255
66. Hardison, W. G., and Weiner, R. (1980) Taurine transport by rat hepatocytes in primary culture. *Biochim. Biophys. Acta* **598,** 145–152
67. Vinnakota, S., Qian, X., Egal, H., Sarthy, V., and Sarkar, H. K. (1997) Molecular characterization and *in situ* localization of a mouse retinal taurine transporter. *J. Neurochem.* **69,** 2238–2250
68. Dominy, J., Jr., Thinschmidt, J. S., Peris, J., Dawson, R., Jr., and Papke, R. L. (2004) Taurine-induced long lasting potentiation in the rat hippocampus shows a partial dissociation from total hippocampal taurine content and independence from activation of known taurine transporters. *J. Neurochem.* **89,** 1195–1205
69. Sturman, J. A., Rassin, D. K., Hayes, K. C., and Gaull, G. E. (1978) Taurine deficiency in the kitten. Exchange and turnover of [^{35}S]taurine in brain, retina, and other tissues. *J. Nutr.* **108,** 1462–1476
70. Saiki, H., Chan, E. T., Wong, E., Yamamuro, W., Ookhtens, M., and Kaplowitz, N. (1992) Zonal distribution of cysteine uptake in the perfused rat liver. *J. Biol. Chem.* **267,** 192–196
71. Bella, D. L., Hirschberger, L. L., Kwon, Y. H., and Stipanuk, M. H. (2002)

Cysteine metabolism in periportal and perivenous hepatocytes. Perivenous cells have greater capacity for glutathione production and taurine synthesis but not for cysteine catabolism. *Amino Acids* **23,** 453–458
72. Parsons, R. B., Ramsden, D. B., Waring, R. H., Barber, P. C., and Williams, A. C. (1998) Hepatic localization of rat cysteine dioxygenase. *J. Hepatol.* **29,** 595–602
73. Lopez-Corcuera, B., Liu, Q. R., Mandiyan, S., Nelson, H., and Nelson, N. (1992) Expression of a mouse brain cDNA encoding novel γ-aminobutyric acid transporter. *J. Biol. Chem.* **267,** 17491–17493
74. Burnham, C. E., Buerk, B., Schmidt, C., and Bucuvalas, J. C. (1996) A liver-specific isoform of the betaine/GABA transporter in the rat. cDNA sequence and organ distribution. *Biochim. Biophys. Acta* **1284,** 4–8
75. White, H. L. (1981) Glutamate as a precursor of GABA in rat brain and peripheral tissues. *Mol. Cell. Biochem.* **39,** 253–259
76. Roberts, E., and Bregoff, H. M. (1953) Transamination of γ-aminobutyric acid and β-alanine in brain and liver. *J. Biol. Chem.* **201,** 393–398
77. Ferenci, P., Stehle, T., Ebner, J., Schmid, R., and Häussinger, D. (1988) Uptake and catabolism of γ-aminobutyric acid by the isolated perfused rat liver. *Gastroenterology* **95,** 402–407
78. Qume, M., and Fowler, L. J. (1996) Effects of chronic oral treatment with GABA-transaminase inhibitors on the GABA system in brain, liver, kidney, and plasma of the rat. *Biochem. Pharmacol.* **52,** 1355–1363
79. Schafer, D. F., Fowler, J. M., and Jones, E. A. (1981) Colonic bacteria. A source of γ-aminobutyric acid in blood. *Proc. Soc. Exp. Biol. Med.* **167,** 301–303
80. Sergeeva, O. A., Chepkova, A. N., Doreulee, N., Eriksson, K. S., Poelchen, W., Mönnighoff, I., Heller-Stilb, B., Warskulat, U., Häussinger, D., and Haas, H. L. (2003) Taurine-induced long lasting enhancement of synaptic transmission in mice. Role of transporters. *J. Physiol.* **550,** 911–919
81. Sergeeva, O. A., Fleischer, W., Chepkova, A. N., Warskulat, U., Häussinger, D., Siebler, M., and Haas, H. L. (2007) $GABA_A$-receptor modification in taurine transporter knockout mice causes striatal disinhibition. *J. Physiol.* **585,** 539–548
82. Chiu, C. S., Jensen, K., Sokolova, I., Wang, D., Li, M., Deshpande, P., Davidson, N., Mody, I., Quick, M. W., Quake, S. R., and Lester, H. A. (2002) Number, density, and surface/cytoplasmic distribution of GABA transporters at presynaptic structures of knock-in mice carrying GABA transporter subtype 1-green fluorescent protein fusions. *J. Neurosci.* **22,** 10251–10266
83. Lehre, K. P., and Rusakov, D. A. (2002) Asymmetry of Glia near central synapses favors presynaptically directed glutamate escape. *Biophys. J.* **83,** 125–134
84. Lehre, K. P., and Danbolt, N. C. (1998) The number of glutamate transporter subtype molecules at glutamatergic synapses. Chemical and stereological quantification in young adult rat brain. *J. Neurosci.* **18,** 8751–8757
85. Furness, D. N., Dehnes, Y., Akhtar, A. Q., Rossi, D. J., Hamann, M., Grutle, N. J., Gundersen, V., Holmseth, S., Lehre, K. P., Ullensvang, K., Wojewodzic, M., Zhou, Y., Attwell, D., and Danbolt, N. C. (2008) A quantitative assessment of glutamate uptake into hippocampal synaptic terminals and astrocytes. New insights into a neuronal role for excitatory amino acid transporter 2 (EAAT2). *Neuroscience* **157,** 80–94
86. Holmseth, S., Dehnes, Y., Huang, Y. H., Follin-Arbelet, V. V., Grutle, N. J., Mylonakou, M. N., Plachez, C., Zhou, Y., Furness, D. N., Bergles, D. E., Lehre, K. P., and Danbolt, N. C. (2012) The density of EAAC1 (EAAT3) glutamate transporters expressed by neurons in the mammalian CNS. *J. Neurosci.* **32,** 6000–6013
87. Bismuth, Y., Kavanaugh, M. P., and Kanner, B. I. (1997) Tyrosine 140 of the γ-aminobutyric acid transporter GAT-1 plays a critical role in neurotransmitter recognition. *J. Biol. Chem.* **272,** 16096–16102
88. Yamashita, A., Singh, S. K., Kawate, T., Jin, Y., and Gouaux, E. (2005) Crystal structure of a bacterial homologue of Na^+/Cl^--dependent neurotransmitter transporters. *Nature* **437,** 215–223
89. Beckstrøm, H., Bjørnsen, L. P., Arancibia, S., Tapia-Arancibia, L., and Danbolt, N. C. (2001) Immobilization stress increases the hippocampal protein levels of the GABA transporter GAT1. *J. Neurochem.* **78,** S37

Deletion of the γ-Aminobutyric Acid Transporter 2 (GAT2 and SLC6A13) Gene in Mice Leads to Changes in Liver and Brain Taurine Contents

Yun Zhou, Silvia Holmseth, Caiying Guo, Bjørnar Hassel, Georg Höfner, Henrik S. Huitfeldt, Klaus T. Wanner and Niels C. Danbolt

J. Biol. Chem. 2012, 287:35733-35746.
doi: 10.1074/jbc.M112.368175 originally published online August 15, 2012
